RESEARCH ARTICLE

Fabrication and optimization of ZnO-multiwalled carbon nanotubes modified glassy carbon electrode for the detection of 2-(4-(1-isonicotinoyl-5-aryl-4,5-dihydro-1*H*-pyrazol-3-yl) phenoxy)-*N*-arylacetamides

Gagandeep Kour Reen[1,2] · Ashok Kumar[1] · Pratibha Sharma[1]

Abstract

A series of 2-(4-(1-isonicotinoyl-5-aryl-4,5-dihydro-1*H*-pyrazol-3-yl)phenoxy)-*N*-arylacetamides has been synthesized in appreciable yields. The quantitative determination and redox behavior of the synthesized compounds were estimated by cyclic voltammetry (CV). Further, it was observed that nanocomposites have come to be the superior modifying materials for electrochemical sensing. Herein, a highly sophisticated and sensitive zinc oxide (ZnO)-multi walled carbon nanotubes (MWCNTs) composite film modified glassy carbon electrode (GCE) (ZnO-MWCNTs/GCE) was fabricated for its use as the working electrode. Prior to the fabrication, the synthesized ZnO material was characterized by SEM to confirm the successful synthesis. After the fabrication of the ZnO-MWCNTs/GCE sensor, it together with its corresponding forms i.e., ZnO/GCE and MWCNTs/GCE including bare GCE was characterized by voltammetry. The increase in effective surface area of modified GCE from that of unembellished GCE of 0.0314 cm^2 up to 0.081 cm^2 resulted in better electrocatalytic activity in terms of responses of the compounds under investigation. The composite film modified GCE resulted in an excellent sensor for the reported compounds in terms of low potential detection, a low detection limit, fast and clear response. Moreover, the effect of pH, varying scan rates, solvents, electrolytes, concentration, and substituents (in terms of the Hammett equation) have also been analyzed on the CV responses of the modified GCE. The best results were obtained for a pH value corresponding to 5.83 with TEAP as the surfactant at the scan rate of 0.1 V/s. The incorporation of ZnO nanoparticles with multi walled carbon nanotubes (MWCNTs) greatly increases the voltammetric peak current and electrochemical reactivity of the compounds. The electrochemical sensor shows sensitivity par excellence and exhibits a wide detection range varying from 1.0×10^{-4} to 3.0×10^{-4} M. Moreover, the detection limit is 1.25×10^{-6} M with a correlation coefficient (r^2) of 0.994. The studies delineated the diffusion-controlled and irreversible behavior of electrocatalytic reaction for all the compounds under investigation.

✉ Pratibha Sharma
  drpratibhasharma@yahoo.com

1   School of Chemical Sciences, Devi Ahilya Vishwavidyalaya, Indore, M.P., India

2   Jawaharlal Nehru Govt. Degree College, Barwaha, M.P., India

Graphic Abstract
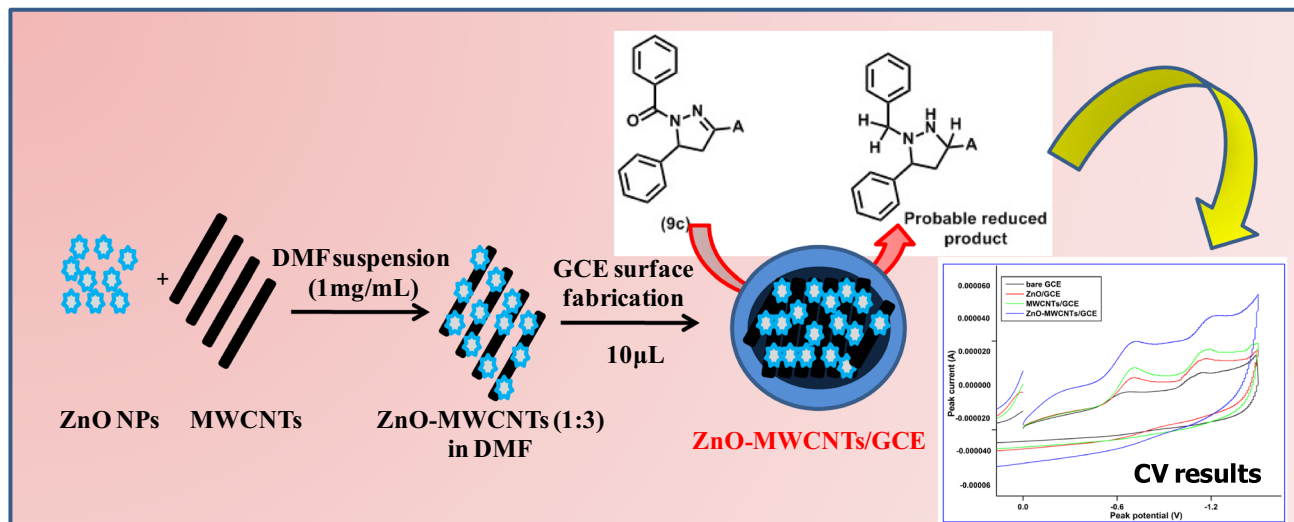
Keywords Cyclic voltammetry · Chemically modified electrode · Sensor · SEM · Diffusion-controlled · Hammett equation

1 Introduction

Electrochemistry constitutes one of the fundamental domains of analytical chemistry [1]. During the past decades, modern electrochemical techniques have been widely used for the determination of pharmaceuticals and other analytes. Cyclic Voltammetry (CV) has been observed to be a most effective, popular, and reliable electrochemical technique on account of its capability to determine the thermodynamics of redox processes, effect of media on these processes, the kinetics of electron-transfer reactions, and coupled chemical reactions [2–5]. This method is highly selective and sensitive as the analyte can be readily identified even in its trace amounts by its voltammetric peak potential [6]. Conclusively, electrochemistry has been evolved as a unique tool to provide significant information for the presence of a material in trace amounts, the redox behavior and number of electrons involved in these reactions.

Furthermore, recent years have witnessed the excessive use of chemically modified electrodes (CMEs), possessing a wide arena of electrochemical functions. The CMEs exhibited afresh chemical, physical, electrochemical, and transport properties [7]. Well designed and fabricated CMEs with high surface area resulted in highly sensitive and selective electrochemical sensors, which played a prominent role in electroanalysis.

A review of the literature delineated the use of different materials in the modification of glassy carbon electrode (GCE). In this regard, multi walled carbon nanotubes (MWCNTs), graphene, graphene oxide, metal oxides, ionic liquids, and polymers are some of the worth citing names of electrode surface modifiers [8–11]. Among various carbonaceous materials, MWCNTs have gained attraction owing to their admirable electrical and mechanical properties. Moreover the high stability and larger surface area resulted into its application as promising material in several fields including its use as electrochemical sensors [12]. In particular, among different metal oxides, zinc oxide (ZnO) is a promising material for electroanalytical studies owing to its low-cost, biocompatibility, non-toxicity, high thermal stability, and piezoelectric behavior. Several studies have delineated the role of ZnO as an efficient electrochemical sensor [13]. Recent studies revealed the enhancement in electrocatalytic activity in terms of enhanced electroactive surface area of the electrode and intervened electron transfer among electrode and electrolyte as a consequence of the combined effect of metal oxides with MWCNTs [14–16]. Taking advantage of the unique electronic properties associated with MWCNTs, it is expected that a combination of ZnO nanoparticles (ZnO NPs) with MWCNTs may result into the advancement of the electron transfer rate thereby enhancing the peak currents and electrocatalytic activity of the fabricated sensor in terms of output signal. [17, 18]

Likewise, the addition of surface-active agents (surfactants) has played an effective role in the electroanalysis of biologically active compounds and drugs [19].

The prerequisite for a surfactant is its adsorption at the interface between electrode and solution. Literature has unveiled the role of surfactants in influencing the kinetics of electron transfer thereby controlling the electrochemical reactions. Surfactants could modify and control the properties of electrode surfaces and provide a specific orientation of the molecules at the electrode surface to enhance the productivity of electrochemical investigations [20–23].

In addition, there is currently no report available for the cyclic voltammetric analyses of the moieties under consideration. This article included a thorough explanation of how to optimize the variables that impacted the voltammetric analysis and the outcomes. The modified GCE worked well as a sensor to identify molecules with these kinds of moieties, which was useful for subsequent study. Buoyed from these studies present work provide an account of nano ZnO-MWCNTs composite film modified GCE (ZnO-MWCNTs/GCE) for electrochemical investigations of 2-(4-(1-isonicotinoyl-5-aryl-4,5-dihydro-1*H*pyrazol-3-yl) phenoxy)-*N*-arylacetamides. Also, the sensitivity of developed sensor was compared with the three electrodes i.e., GCE, ZnO/GCE and MWCNTs/GCE for the analysis of the compounds. The results favored the higher activity/sensitivity of ZnO-MWCNTs/GCE.

2 Experimental section

All chemicals were purchased from commercial suppliers and used without further purification. The reactions were performed in an aerobic atmosphere without any specific precautions. Melting points were determined on a Veego melting-point apparatus and were uncorrected. Fourier Transform Infra-Red (FTIR) spectra were recorded within the range of 4000–400 cm^{-1} using Frontier Perkin-Elmer FTIR SP 10 STD. The ^{1}H and ^{13}C NMR spectra of the synthesized compounds were recorded at 400 and 100 MHz, respectively using Bruker Avance II 400 NMR spectrometer using deuterated chloroform (CDCl$_3$) as the solvent, and the chemical shifts were expressed in parts per million (ppm). Spin multiplicities were described as s (singlet), d (doublet), t (triplet), q (quartet), and m (multiplet). Mass spectra were recorded on a quadruple-time-of-flight (Q-TOF) mass spectrometer (MICROMASS) using electrospray ionization (ESI) in positive mode. Scanning Electron Microscopic (SEM) images and their corresponding Electron Dispersive X-ray analysis (EDX) data were recorded by Jeol microscope (JSM7100F). Elemental analyses were performed on Thermo Scientific (Flash 2000) CHN Elemental Analyzer. Thin-layer chromatography (TLC) was carried out using precoated aluminum sheets with silica gel-60 F254 (Scheme 1).
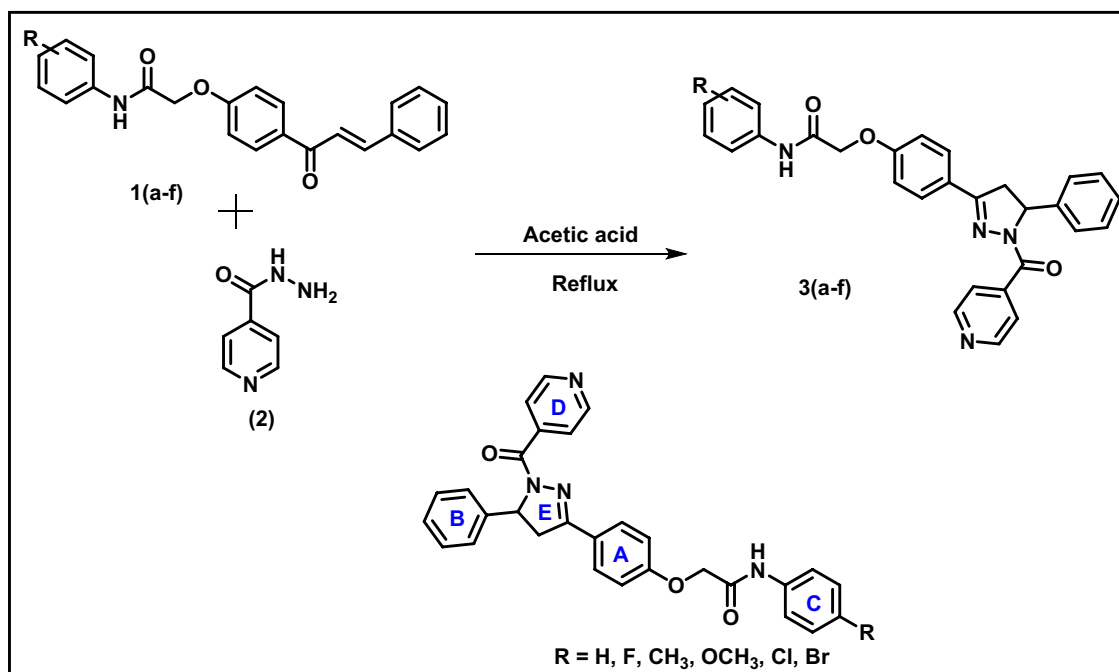
Scheme 1 Synthetic procedure for the synthesis of 2-(4-(1-isonicotinoyl-5-phenyl-4,5-dihydro-1H-pyrazol-3-yl)) derivatives (**3a–f**)

2.1 General procedure for synthesis of 2-(4-(1-isonicotinoyl-5-phenyl-4,5-dihydro-1H-pyrazol-3-yl)) derivatives (3a-f)

Pertinent *N*-phenylacetamide derivatives (1a–o, 1 mmol) [24] and isoniazid (0.165g, 1.2 mmol) were taken in a 50 c.c. round-bottomed flask containing 5 mL of acetic acid. The mixture was refluxed and the progress was monitored by TLC (petroleum ether: ethyl acetate in 3:2). After completion of the reaction ice-cold water was added, precipitate obtained was washed with water and then with acetone to obtain a solid product in pure form.

2.1.1 2-(4-(1-Isonicotinoyl-5-phenyl-4,5-dihydro-1H-pyrazol-3-yl)phenoxy)-N-phenylacetamide (3a)

Prepared from (E)-2-(4-cinnamoylphenoxy)-N-phenylacetamide (**1a**, 0.357g, 1 mmol); light yellow powder; Yield: 82%; m.p. 74–76 °C; FTIR ($\bar{v}$, cm^{-1}) 3168 (N–H), 3098 (C–H, sp^2), 2978, 2856 (C–H, sp^3), 1662 (NH–C=O), 1648 (C=N), 1566, 1495 (C----C, ring str.), 1466 (CH$_2$, bend), 1345 (C–N, ring), 1220 (C–O–C), 850, 745 (sub. Phenyl, sp^2 C–H bend); ^{1}H NMR (400 MHz, DMSO-d6) δ 8.76 (*d*, 2H, *J* = 8 Hz, H-32,34, Ring D), 8.21 (*d*, 2H, *J* = 12 Hz, H-14,16, Ring A), 8.09 (*d*, 2H, *J* = 8 Hz, H-31,35, Ring D), 7.70–7.63 (*m*, 2H, H-6,10, Ring C), 7.59–7.53 (*m*, 2H, H-24,28, Ring B), 7.35–7.28 (*m*, 6H, Ring B & C), 7.05 (*d*, 2H, *J* = 12 Hz, H-13,17, Ring A), 5.80 (*dd*, 1H, H-22, Ring E), 4.70 (*s*, 2H, CH$_2$), 3.75 (*dd*, 1H, H-21, Ring E), 3.19 (*dd*, 1H, H-21', Ring E); ^{13}C NMR (100 MHz, DMSO-d6) δ 167.8, 167.1, 160.6, 151.9, 149.4, 141.9, 140.8, 138.7, 129.1, 128.5, 128.8, 128.1, 126.8, 126.6, 121.8, 121.5, 114.5, 66.8, 66.5, 40.1; HRMS m/z [M+H]$^+$: 477.54; Anal. Calcd. for C$_{29}$H$_{24}$N$_4$O$_3$: C, 73.09, H, 5.08, N, 11.76. Found C, 73.11, H, 5.09, N, 11.79.

2.1.2 N-(4-fluorophenyl)-2-(4-(1-isonicotinoyl-5-phenyl-4,5-dihydro-1H-pyrazol-3-yl)phenoxy)acetamide (3b)

Prepared from (E)-2-(4-cinnamoylphenoxy)-N-(4-fluorophenyl)acetamide (**1b**, 0.375g, 1 mmol); light yellow powder; Yield: 84%; m.p. 138–140 °C; FTIR ($\bar{v}$, cm^{-1}) 3411 (N–H), 3098 (C–H, sp2), 2978, 2856 (C–H, sp^3), 1674 (NH–C=O), 1658 (C=N), 1566, 1495 (C----C, ring str.), 1446 (CH$_2$, bend), 1345 (C–N, ring), 1232 (C–O–C), 850, 745 (sub. Phenyl, sp^2 C–H bend); ^{1}H NMR (400 MHz, DMSO-d6) δ 8.77 (*d*, 2H, *J* = 12 Hz, H-32,34, Ring D), 8.53 (*s*, 1H, NH), 8.25 (*d*, 2H, *J* = 8 Hz, H-14,16, Ring A), 7.84–7.78 (*m*, 4H, Ring B & C) 7.71 (*d*, 2H, *J* = 12Hz, H-31,35, Ring D), 7.35–7.30 (*m*, 5H, Ring B & C), 7.04 (*d*, 2H, J = 8Hz, H-13,17, Ring A), 5.81 (dd, 1H, H-22, Ring E), 4.68 (*s*, 2H, CH$_2$), 3.83 (*dd*, 1H, H-21, Ring E), 3.25 (*dd*, 1H, H-21', Ring E); ^{13}C

NMR (100 MHz, DMSO-d6) δ 167.9, 167.2, 162.7, 160.3, 151.8, 149.4, 141.0, 140.6, 134.3, 128.8, 128.5, 126.8, 126.6, 121.6, 120.5, 115.1, 114.3, 66.8, 66.6, 40.3; HRMS m/z [M+H]$^+$: 495.24; Anal. Calcd. for C$_{29}$H$_{23}$FN$_4$O$_3$: C, 70.43, H, 4.69, N, 11.33. Found C, 70.41, H, 4.65, N, 11.36.

2.1.3 2-(4-(1-Isonicotinoyl-5-phenyl-4,5-dihydro-1H-pyrazol-3-yl)phenoxy)-N-(p-tolyl)acetamide (3c)

Prepared from (E)-2-(4-cinnamoylphenoxy)-N-(p-tolyl)acetamide (**1c**, 0.371g, 1 mmol); off white powder; Yield: 84%; m.p. 124–126 °C; FTIR ($\bar{v}$, cm^{-1}) 3275 (N–H), 3072 (C–H, sp^2), 2961, 2859 (C–H, sp^3), 1672 (NH–C=O), 1652 (C=N), 1567, 1495 (C----C, ring str.), 1451 (CH$_2$, bend), 1376 (C–N, ring), 1270 (C–O–C), 928, 838, 762 (sub. Phenyl, sp^2 C–H bend); ^{1}H NMR (400 MHz, DMSO-d6) δ 8.75 (*d*, 2H, *J* = 8 Hz, H-32,34, Ring D), 8.10 (*d*, 2H, *J* = 12 Hz, H-14,16, Ring A), 7.82 (*d*, 2H, *J* = 8 Hz, H-31,35, Ring D), 7.47–7.41 (*m*, 4H, Ring C), 7.24–7.17 (*m*, 5H, Ring B), 7.04–7.01 (*d*, 2H, *J* = 12 Hz, H-13,17, Ring A), 5.78 (*dd*, 1H, H-22, Ring E), 4.69 (*s*, 2H, CH$_2$), 3.83 (*dd*, 1H, H-21, Ring E), 3.25 (*dd*, 1H, H-21', Ring E); ^{13}C NMR (100 MHz, DMSO-d6) δ 167.7, 167.3, 160.2, 151.6, 149.8, 141.8, 140.7, 136.7, 135.3, 129.3, 128.8, 128.5, 126.9, 126.6, 121.8, 121.6, 114.5, 66.8, 66.5, 39.7, 21.2; HRMS m/z [M+H]$^+$: 491.51; Anal. Calcd. for C$_{30}$H$_{26}$N$_4$O$_3$: C, 73.45, H, 5.34, N, 11.42. Found C, 73.41, H, 5.36, N, 11.39.

2.1.4 2-(4-(1-Isonicotinoyl-5-phenyl-4,5-dihydro-1H-pyrazol-3-yl)phenoxy)-N-(4-methoxyphenyl)acetamide (3d)

Prepared from (E)-2-(4-cinnamoylphenoxy)-N-(4-methoxyphenyl)acetamide (**1d**, 0.387g, 1 mmol); yellow powder; Yield: 84%; m.p. 158–160 °C; FTIR ($\bar{v}$, cm^{-1}) 3238 (N–H), 3082 (C–H, sp^2), 2946, 2861 (C–H, sp^3), 1669 (NH–C=O), 1651 (C=N), 1579, 1495 (C----C, ring str.), 1442 (CH$_2$, bend), 1368 (C–N, ring), 1268 (C–O–C), 928, 774 (sub. Phenyl, sp^2 C–H bend); ^{1}H NMR (400 MHz, DMSO-d6) δ 8.78 (*d*, 2H, *J* = 12 Hz, H-32,34, Ring D), 8.16 (*d*, 2H, *J* = 16 Hz, H-14,16, Ring A), 7.99 (*d*, 2H, *J* = 12 Hz, H-31,35, Ring D), 7.47–7.41 (*m*, 4H, Ring B & C), 7.10–7.03 (*m*, 3H, Ring B), 6.97 (*d*, 2H, *J* = 16 Hz, H-13,17, Ring A), 6.81–6.77 (*m*, 2H, Ring C), 5.77 (*dd*, 1H, H-22, Ring E), 4.64 (*s*, 2H, CH$_2$), 3.75–3.70 (*m*, 4H, OCH$_3$ & H-21, Ring E) 3.19 (*dd*, 1H, H-21', Ring E); ^{13}C NMR (100 MHz, DMSO-d6) δ 167.6, 167.1, 160.6, 158.9, 151.5, 149.7, 141.5, 140.8, 130.9, 128.7, 128.6, 126.7, 126.4, 122.6, 121.7, 114.6, 114.1, 66.9, 66.5, 55.8, 39.9; HRMS m/z [M+H]$^+$: 507.53; Anal. Calcd. for C$_{30}$H$_{26}$N$_4$O$_4$: C, 71.13, H, 5.17, N, 11.06. Found C, 71.15, H, 5.19, N, 11.09.

2.1.5 N-(4-bromophenyl)-2-(4-(1-isonicotinoyl-5-phenyl-4,5-dihydro-1H-pyrazol-3-yl)phenoxy)acetamide (3e)

Prepared from (E)-N-(4-bromophenyl)-2-(4-cinnamoylphenoxy)acetamide (**1e**, 0.436g, 1 mmol); off white powder; Yield: 86%; m.p. 140–142 °C; FTIR ($\bar{v}$, cm^{-1}) 3334 (N–H), 3102 (C–H, sp^2), 2976, 2867 (C–H, sp^3), 1671 (NH–C=O), 1652 (C=N), 1591, 1487 (C----C, ring str.), 1457 (CH$_2$, bend), 1357 (C–N, ring), 1235 (C–O–C), 898, 756 (sub. Phenyl, sp^2 C–H bend); ^{1}H NMR (400 MHz, DMSO-d6) δ 8.88 (d, 2H, J = 12 Hz, H-32,34, Ring D), 8.12 (d, 2H, J = 8 Hz, H-14,16, Ring A), 7.81 (d, 2H, J = 12 Hz, H-31,35, Ring D), 7.65–7.61 (m, 2H, H-6,10, Ring C), 7.28–7.23 (m, 5H, Ring B), 6.85–6.80 (m, 4H, Ring A & C), 5.78 (dd, 1H, H-22, Ring E), 4.72 (s, 2H, CH$_2$), 3.79 (dd, 1H, H-21, Ring E), 3.24 (dd, 1H, H-21', Ring E); ^{13}C NMR (100 MHz, DMSO-d6) δ 167.9, 167.2, 161.1, 152.2, 149.8, 141.6, 140.6, 137.6, 131.7, 129.3, 128.6, 128.5, 126.8, 126.5, 121.7, 122.5, 114.5, 66.7, 66.5, 39.8; HRMS m/z [M+H]$^+$: 556.45; Anal. Calcd. for $C_{29}H_{23}BrN_4O_3$: C, 62.71, H, 4.17, N, 10.09. Found C, 62.74, H, 4.19, N, 10.05.

2.1.6 N-(4-chlorophenyl)-2-(4-(1-isonicotinoyl-5-phenyl-4,5-dihydro-1H-pyrazol-3-yl)phenoxy)acetamide (3f)

Prepared from (E)-N-(4-chlorophenyl)-2-(4-cinnamoylphenoxy)acetamide (**1f**, 0.391g, 1 mmol); off white powder; Yield: 84%; m.p. 120–122 °C; FTIR ($\bar{v}$, cm^{-1}) 3297 (N–H), 3084 (C–H, sp^2), 2946, 2854 (C–H, sp^3), 1667 (NH–C=O), 1655 (C=N), 1597, 1494 (C----C, ring str.), 1461 (CH$_2$, bend), 1369 (C–N, ring), 1257 (C–O–C), 945, 686 (sub. Phenyl, sp^2 C–H bend); ^{1}H NMR (400 MHz, DMSO-d6) δ 8.84 (d, 2H, J = 12 Hz, H-32,34, Ring D), 8.09 (d, 2H, J = 8 Hz, H-14,16, Ring A), 7.85 (d, 2H, J = 12 Hz, H-31,35, Ring D), 7.67–7.63 (m, 2H, H-6,10, Ring C), 7.30–7.35 (m, 5H, Ring B), 6.89–6.84 (m, 4H, Ring A & C), 5.80 (dd, 1H, H-22, Ring E), 4.69 (s, 2H, CH$_2$), 3.85 (dd, 1H, H-21, Ring E), 3.28 (dd, 1H, H-21', Ring E); ^{13}C NMR (100 MHz, DMSO-d6) δ 167.8, 167.3, 160.5, 151.7, 149.7, 141.5, 140.9, 136.5, 133.4, 129.3, 128.6, 128.5, 126.8, 126.5, 121.5, 120.5, 114.5, 66.7, 66.5, 39.8; HRMS m/z [M+H]$^+$: 511.95; Anal. Calcd. for $C_{29}H_{23}ClN_4O_3$: C, 68.17, H, 4.54, N, 10.96. Found C, 68.19, H, 4.57, N, 10.94.

2.2 Instrumentation

The cyclic voltammetric (CV) studies were performed using computerized Epsilon-2 BAS (Bioanalytical Systems, West Lafayette, USA) potentiostat with three-electrode assembly. GCE was used as the working electrode, Ag/AgCl as the reference electrode, and platinum wire as the counter electrode. Pure nitrogen was bubbled through the electrolyte to remove dissolved oxygen and a blanket of nitrogen gas was maintained during all the runs. All the pH measurements of buffer solutions were made with the help of the Eutech pH meter, which was calibrated with buffers of known pH, (4.0, 7.0, and 9.0, at 25 °C).

2.3 Fabrication of ZnO-MWCNTs/GCE sensor

ZnO NPs were synthesized following the hydrothermal chemical precipitation method [25]. The morphology of the catalyst was further determined by SEM analysis (Figure 1). SEM images of the catalyst depicted the crystalline nature and flower like structure of the synthesized zinc oxide. The surface of GCE was polished with alumina particles (0.5 µm) on a smooth polishing cloth and then rinsed several times with HPLC grade methanol and double distilled water before use. A homogenous
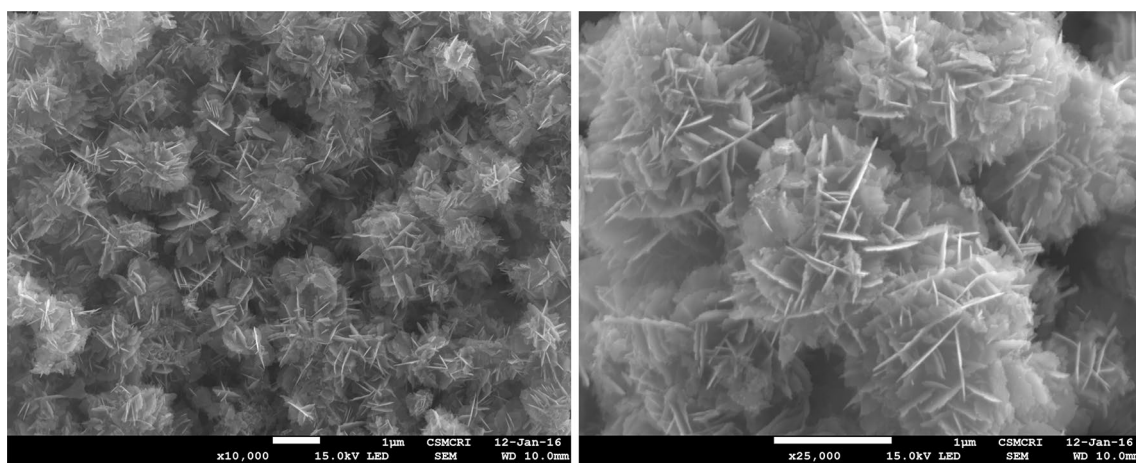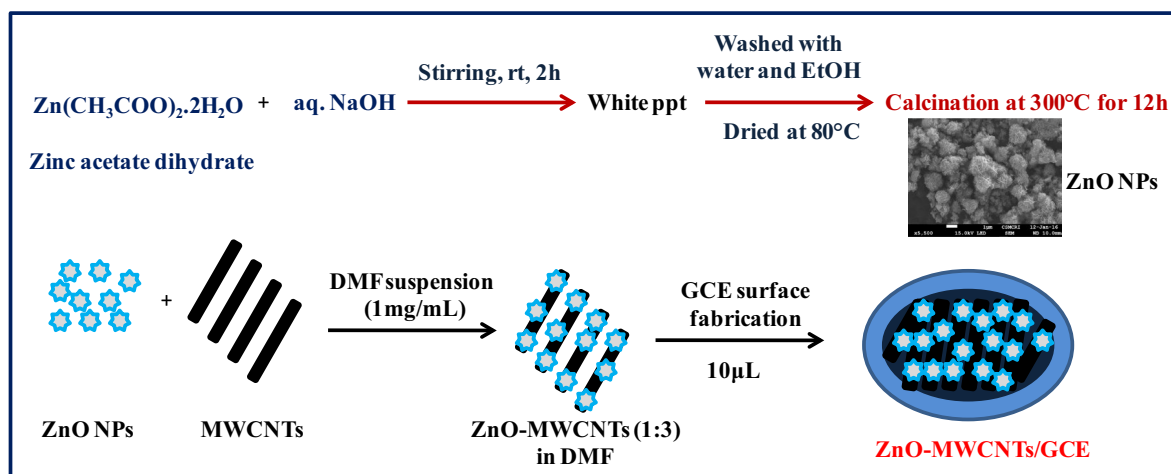

Fig. 1 SEM images showing flowerlike structure

Scheme 2 Fabrication of ZnO-MWCNTs/GCE for voltammetric studies

suspension was prepared by sonicating the mixture of ZnO NPs and MWCNTs in a 1:3 ratio using *N*, *N*-dimethylformamide (DMF) as solvent (1 mg/mL). The known volume (10μL) of ZnO-MWCNTs suspension was dropped onto the GCE surface and then it was air-dried at room temperature to obtain ZnO-MWCNTs/GCE sensor and employed it for voltammetric measurements. Similar suspensions of ZnO NPs and MWCNTs were also prepared in DMF to obtain ZnO/GCE and MWCNTs/GCE for comparative study. The whole process is depicted diagrammatically in Scheme 2.

3 Results and discussion

3.1 Calculation of surface area and performance of hybrid sensors

The effective surface area studies of the fabricated MWC-NTs/GCE, ZnO/GCE, ZnO-MWCNTs/GCE, and bare GCE sensors were performed using a 1.0 mM solution of $K_3[Fe(CN)_6]$ in 0.1 M KCl as redox standard. The slope was calculated by plotting a graph between current (i_p) and the square root of scan rate ($v^{1/2}$) and used for area determination by employing Randles-Savick equation:

$$i_p = \left(2.69 \times 10^5\right) ACD^{1/2} n^{3/2} v^{1/2} \qquad (1)$$

where, *A* is the effective surface area of the electrodes in cm^2, C, D, and n represents the concentration, diffusion coefficient, and the number of electrons, respectively for $K_3[Fe(CN)_6]$ solution. The respective values of n and D for $K_3[Fe(CN)_6]$ solution were 1 and 7.6×10^{-6} cm^2/s [26]. The effective surface area for ZnO-MWCNTs/GCE was calculated to be 0.081 cm^2 which was greater as compared to 0.067 cm^2 for MWCNTs/GCE, 0.051 cm^2 for ZnO/GCE, and

0.0314 cm^2 for bare GCE. Thus, enhancement in the surface area resulted in better electrocatalytic activity than bare GCE in terms of cyclic voltammetric responses of compounds under investigation.

This could be analyzed by carrying out CV analysis for compound **3c** at a scan rate of 0.1 V/s using TEAP as the supporting electrolyte at pH 5.83. The CV peaks (Fig. 2) of **3c** pictured the marked enhancement in peak current values for irreversible reduction peaks to 3.670 and 4.991 at ZnO-MWCNTs/GCE as compared to that encountered for the MWCNTs/GCE as 2.021 and 3.211, respectively.. The order of sensitivity was observed to be in direct correlation with the surface area. Hence, ZnO-MWCNTs/GCE was considered the most promising sensor in comparison to the other hybrid and bare GCE sensors in terms of wonderful
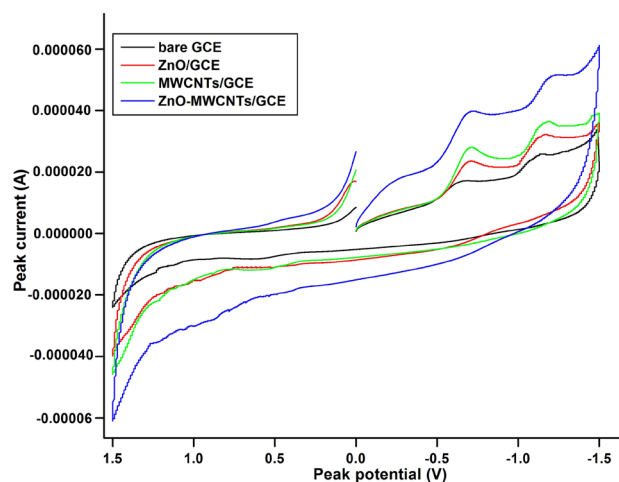

Fig. 2 Comparative study of compound **3c** at different GCE (pH 5.83, Conc. 1×10^{-4} M)

electrical conductivity, rapid electron transmission capacity, and electrocatalytic activity. [18, 27]

3.2 Cyclic voltammetry

To set up the best experimental conditions, the CVs of synthesized compound (**3c**) were recorded at different pH, scan rates from 0.05 V/s to 0.25 V/s, concentrations (1.0×10^{-4} to 3.0×10^{-4} M) and surfactants. All the compounds under investigation exhibited two successive cathodic peaks in the pH range of study (3.50–9.23) for all the scan rates and concentrations. No anodic peak was observed in the reverse scan; thus indicating the total irreversibility of the electrode process. The results of CV indicated the process to be diffusion controlled that could be delineated through:

- The linear relationship between cathodic peak current (i_{pc}) and the square root of scan rate ($\nu^{1/2}$)
- The plot of log i_{pc} vs log ν (with a slope close to 0.5)

Moreover, the irreversible nature of the reaction process could be confirmed by the following facts:

- Absence of anodic peak in the reverse scan
- $E_{p/2c} - E_{pc} > 56.5$ mV

The irreversible nature of the process was further supported by the low transfer coefficient (α) values (< 1.0). The shift of peak potential for both the peaks with a value less than $30/\alpha$ mV under a tenfold increase of scan rate ascertained the irreversible behavior of the reduction process. Following parameters were assessed by CV studies using ZnO-MWCNTs/GCE as a working electrode.

3.2.1 Effect of pH

The pH dependence of synthesized derivative (**3c**) was studied in the pH range of 3.50–9.23 using BR buffers [28], at analyte concentration of 1×10^{-4} M in ACN as solvent and TEAP as supporting electrolyte at a scan rate of 0.1 V/s. The close inspection of data revealed the dependency of peak potential on the pH of the buffer solution. An increase in the value of pH shifted the peak potential towards a more negative value which was the indication of proton participation in the electrode process. At a certain point near pH 7, potential becomes constant because of the decrease in the rate of protonation (Fig. 3). Also, the graph plotted between pH and peak current (Fig. 4) has shown the appreciable increase in peak current upto pH 5.83, followed by a decrease in the value. Moreover, the solution became hazy due to the formation of some precipitate beyond pH 5.83, hence it was found to be optimal for further studies in terms of better peak shape and stable response.

3.2.2 Effect of various solvent and surfactant media

Cyclic voltammetric response of synthesized derivatives was analyzed in different organic solvents (ACN, DMF, and EtOH) and the presence of different surfactants (a non-ionic, a cationic, and an anionic) for pH 5.83 at 0.1 V/s. The analysis of comparative CVs delineated the use of ACN to be the best solvent system. Moreover, the addition of surfactant was found to be more effective in producing precise and clear CV responses. Especially, the use of cationic surfactant TEAP has shown a substantial increase in peak current with a negative shift in the peak potential. It was realized that the peak current responses in non-ionic and anionic surfactant media were observed to be less promising in comparison
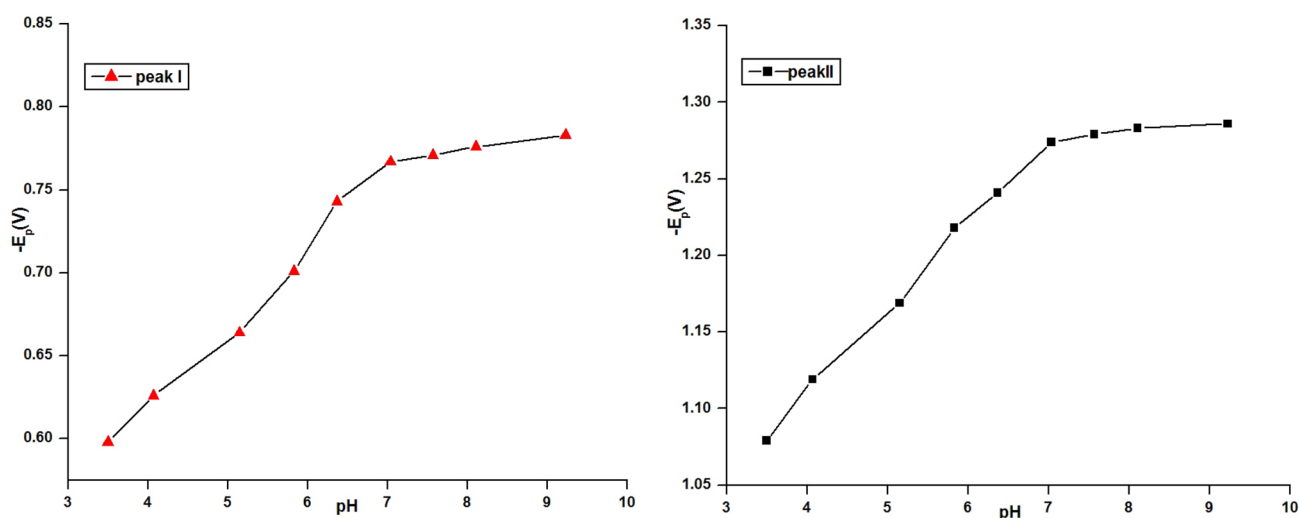

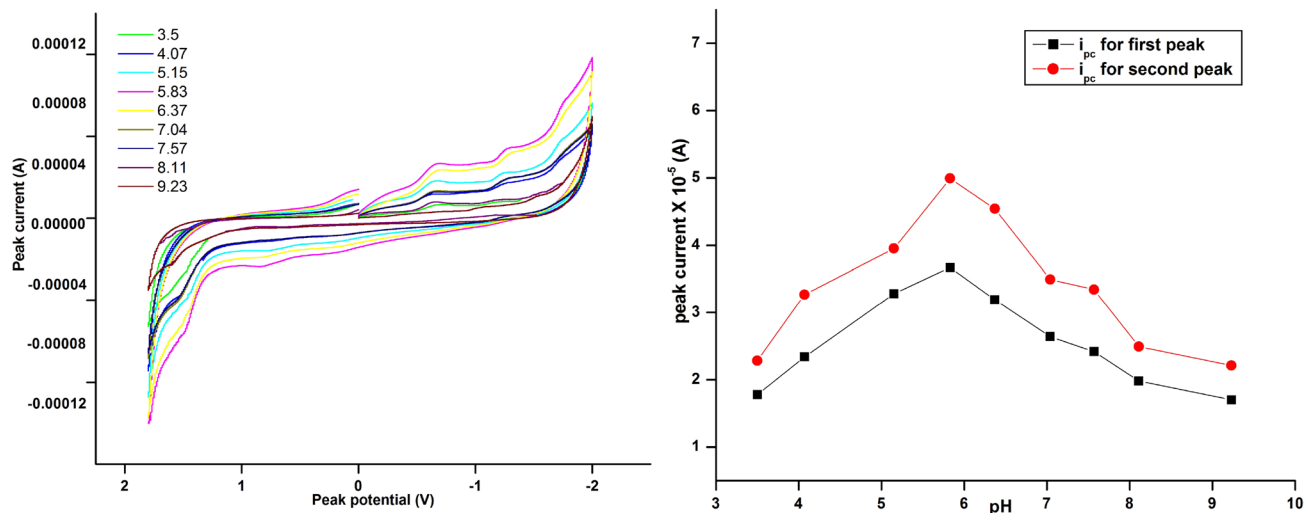**Fig. 3** Effect of pH on peak potentials of **3c** (scan rate 0.1 V/s, Conc. 1×10^{-4} M)

Fig. 4 Effect of pH on peak currents of **3c** (scan rate 0.1 V/s, Conc. 1×10^{-4} M)
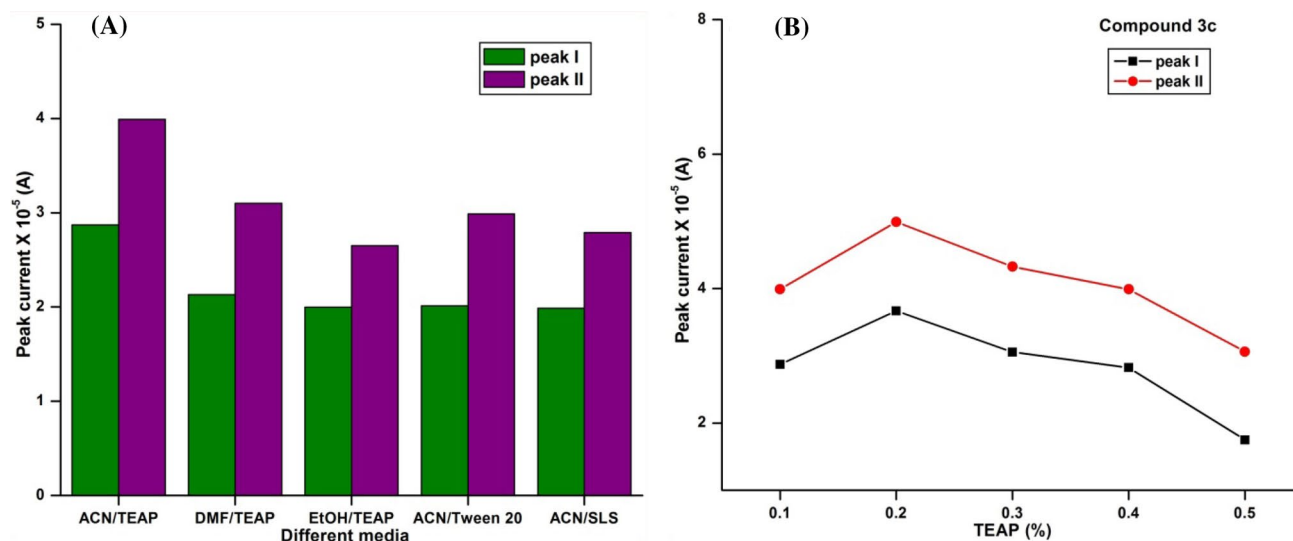

Fig. 5 Peak current response: **A** comparison in different solvent/surfactant media (Conc. 1×10^{-4} M, pH 5.83, scan rate 0.1 V/s); **B** effect of varying concentration of TEAP

to TEAP (cationic surfactant). Cathodic peak responses of derivative **3c** are depicted in Fig. 5A. Thus, ACN has opted as solvent medium and TEAP as the surfactant of choice for electroanalysis of all the derivatives under consideration.

Further, the effect of TEAP concentration on electrochemical reduction of **3c** at GCE was investigated (Fig. 5B). The value of peak current was enhanced as the concentration of TEAP was increased from 0.1% to 0.2%. However, the value of cathodic peak current decreased as the concentration of TEAP exceeded 0.2%. Therefore, a 0.2% aqueous solution of TEAP was found to be optimal for these voltammetric studies.

3.2.3 Effect of varying analyte concentration on CV response

The variation of cathodic peak current was studied at different concentrations of the analyte. Plots between the cathodic peak currents (i_{pc}) and concentrations (C) of analyte ($1.0—3.0 \times 10^{-4}$ M) at scan rate 0.1 V/s, depicted a linear dependence on concentrations (C) for all the six compounds (Fig. 6). A linear correlation obtained between peak current and the analyte concentration signifies that the reduction process was diffusion controlled.
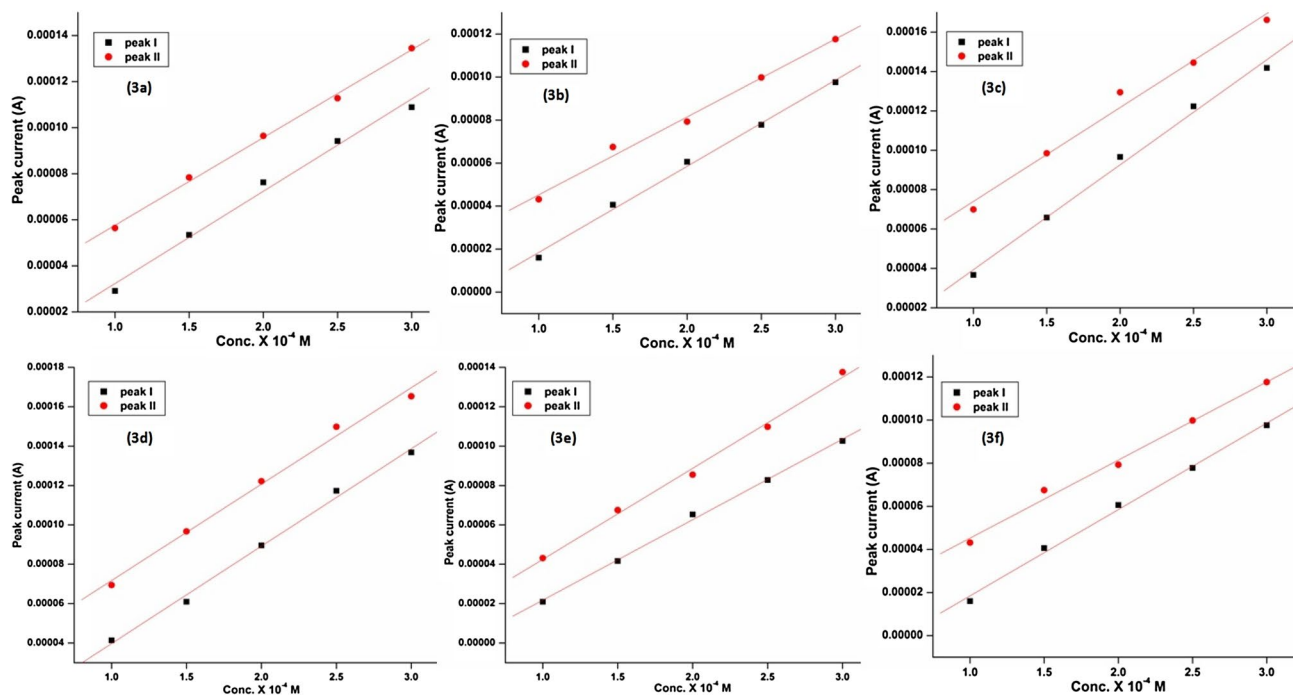
Fig. 6 Plots of peak current i_{pc} (A) *vs* concentration at scan rate 0.1 V/s, (pH 5.83, $A = 0.081$ cm.^{2})

At the analyte concentration of 2×10^{-4} M the peaks obtained were clearly defined and thereby this concentration was selected for further analysis of all the compounds under investigation (Table 1). Moreover, the detection limit was observed to be 1.25×10^{-6} M for seven replicate determinations with correlation coefficient (r^2) as 0.994. The relative standard deviation does not exceed 1.4%.

3.2.4 Effect of varying scan rate on CV response

The voltammetric investigations at various scan rates (0.05–0.25 V/s) were performed under the optimum condition of pH, solvent, surfactant medium, and analyte concentration. CV scans of compound **3c** prepared in TEAP were recorded at a concentration of 2.0×10^{-4} M in B.R. buffer solution of pH 5.83 using ACN as the solvent. The scans obtained at ZnO-MWCNTs/GCE were shown in Fig. 7. Cyclic voltammograms exhibited two cathodic (reduction) peaks at all scan rates for the synthesized derivative **3c**. No anodic peak in the reverse scan was observed for all the compounds. As the scan rate increases gradually from 50 mV/s to 250 mV/s at a fixed concentration of **3c**, the peak potential was shifted towards a more negative value with an increment in the current value.

The signal-to-noise ratio was maximum at a scan rate of 100 mV/s; thus it was chosen to be the optimum scan rate for analyses of all other compounds. The resultant values of peak potential and current at varied scan rates for all six compounds are presented in Table 2.

The graph plotted between peak currents and the square root of scan rate for all the six compounds under investigation (**3a-f**) exhibited a linear correlation between them and thereby revealed the reaction to be diffusion controlled (Fig. 8). Furthermore, the plot of log i_p vs log v resulted in a straight line which can be expressed by the linear equation mentioned in Table 3. The slope for all the compounds was close to the theoretically expected value of 0.5, indicative of a diffusion-controlled electrode process [26].

Moreover, for a typical diffusion-controlled irreversible electrode process, the relationship between E_p and ln v obeys the following equation

$$E_p = E^{\circ} + (RT/\alpha nF)\ln\left(RTk^{\circ}/\alpha nF\right) + (RT/\alpha nF)\ln v \quad (2)$$

where E° stands for formal potential, k° is the standard rate constant of the reaction, α is the charge transfer coefficient, n represents the number of electrons and v is the scan rate. All other symbols have their usual meanings. The graph plotted between E_p and ln v in the range of 50–250 mV/s, resulted in a straight line for all the six compounds under analysis. The linear equation obtained from this correlation was found to be in the following format:

Table 1 Values of $(-E_{pc}, V)$ and (i_{pc}, A) for compound **3c** at different concentration (pH 5.83, $A = 0.081$ cm^2, $\nu = 0.1$ V/s, TEAP)

S. No	Analyte code	R_1	Conc. X 10^{-4} (M)	$-E_{pcI}$ (V)	$-E_{pcII}$ (V)	$i_{pcI} \times 10^{-5}$ (A)	$i_{pcII} \times 10^{-5}$ (A)
1	**3a**	H	1	0.698	1.216	2.91	3.641
			1.5	0.732	1.237	3.341	5.840
			2	0.753	1.253	5.629	7.643
			2.5	0.779	1.285	7.420	9.280
			3	0.794	1.299	8.890	11.450
2	**3b**	4-F	1	0.678	1.179	1.600	2.312
			1.5	0.701	1.204	2.061	4.750
			2	0.735	1.235	4.062	5.927
			2.5	0.756	1.257	5.782	7.980
			3	0.782	1.281	7.760	9.760
3	**3c**	4-CH$_3$	1	0.701	1.218	3.670	4.991
			1.5	0.738	1.246	4.582	7.851
			2	0.766	1.266	7.662	10.942
			2.5	0.789	1.281	10.230	12.450
			3	0.806	1.308	12.180	14.620
4	**3d**	4-OCH$_3$	1	0.736	1.236	2.134	4.943
			1.5	0.754	1.259	4.092	7.670
			2	0.781	1.291	6.954	10.218
			2.5	0.805	1.316	9.730	12.981
			3	0.833	1.347	11.680	14.530
5	**3e**	4-Cl	1	0.632	1.167	1.096	2.311
			1.5	0.678	1.194	2.163	4.754
			2	0.695	1.225	4.531	6.551
			2.5	0.721	1.59	6.280	8.980
			3	0.746	1.84	8.260	11.760
6	**3f**	4-Br	1	0.615	1.157	1.895	2.814
			1.5	0.646	1.197	2.461	5.051
			2	0.679	1.220	4.987	6.982
			2.5	0.698	1.571	6.584	8.480
			3	0.728	1.597	8.160	11.920

$$E_p = \text{slope} \times \ln\nu + \text{intercept} \tag{3}$$

Thus from Eqs. 2 and 3, the following correlation is obtained:

$$(RT/\alpha nF) = \text{slope} \tag{4}$$

where, $T = 298$ K, $R = 8.314$ J K^{-1} mol^{-1} and $F = 96{,}500$ C. For an irreversible system, the value of α was assumed to be 0.5. Thus with the help of Eq. 4, the number of electrons involved in the reduction process was evaluated. The number of electrons involved in reduction corresponding to the peak I and peak II were calculated to be 2 and 4, respectively.

The potential at half of the peak current value is known as half peak potential ($E_{p/2}$). For a wave that is irreversible, E_p is a function of scan rate whose value gets shifted in a negative direction (for reduction) by a value less than $30/\alpha$ mV, when the increase of scan rate is under tenfold value.

Moreover, the relationship for E_p, $E_{p/2}$ and charge transfer coefficient (α) for an irreversible system is governed by Eq. 5 [29].

$$E_p - E_{p/2} = 1.857(RT/\alpha F) \text{ or } 0.0477/\alpha \, V \tag{5}$$

Thus, definite values of α could be calculated from this equation and are presented in Table 4. The value of α is found to be closer to 0.5 for all the six compounds; thus governing the irreversible nature of the reduction process.

The values of the diffusion coefficient for all the analytes were determined using Eq. 6, in accordance with the diffusion-controlled behavior of electrode process [26]:

$$i_p = (2.99 \times 10^5) \, n. \, \alpha^{1/2}. \, A. \, C. \, D_0^{1/2}. \, \nu^{1/2} \tag{6}$$

where, i_p = peak current in ampere, n = number of electrons, α = charge transfer coefficient, A = area of the electrode in
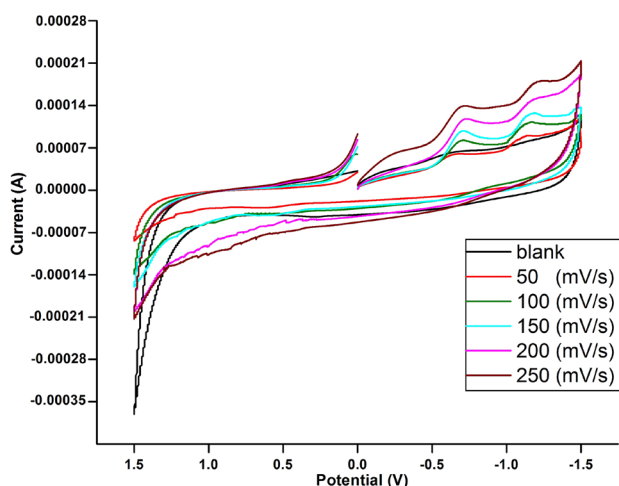
Fig. 7 Cyclic voltammograms of 2-(4-(1-isonicotinoyl-5-phenyl-4,5-dihydro-1H-pyrazol-3-yl)phenoxy)-N-(p-tolyl)acetamide (**3c**) at different scan rates (0.05–0.25 V/s) at ZnO-MWCNTs/GCE (pH 5.83, $C = 2.0 \times 10^{-4}$ M)

cm^2, $D_0 =$ diffusion coefficient of the species in $cm^2 s^{-1}$, $v =$ scan rate in V/s, $C =$ Molar concentration of the analyte in solution.

The forward rate constant for a diffusion-controlled, irreversible electrode process was determined using Eq. 7.

$$E_p = -RT/\alpha F \left[0.780 + \ln\left(D_0^{1/2}/k^0\right) + \ln\left(\alpha F v/RT\right)^{1/2}\right]$$

(7)

where, R, T, and F have their usual values, $E_p =$ peak potential in Volts, $k^\circ =$ forward rate constant cm/s.

The values of the diffusion coefficient and forward rate constant for both the waves are mentioned in Table 5.

3.2.5 Effect of substituents (Hammett equation):

The effect of substituents on the reduction of electroactive species was studied and analyzed as per the well known modified Hammett equation expressed as follows [30]:
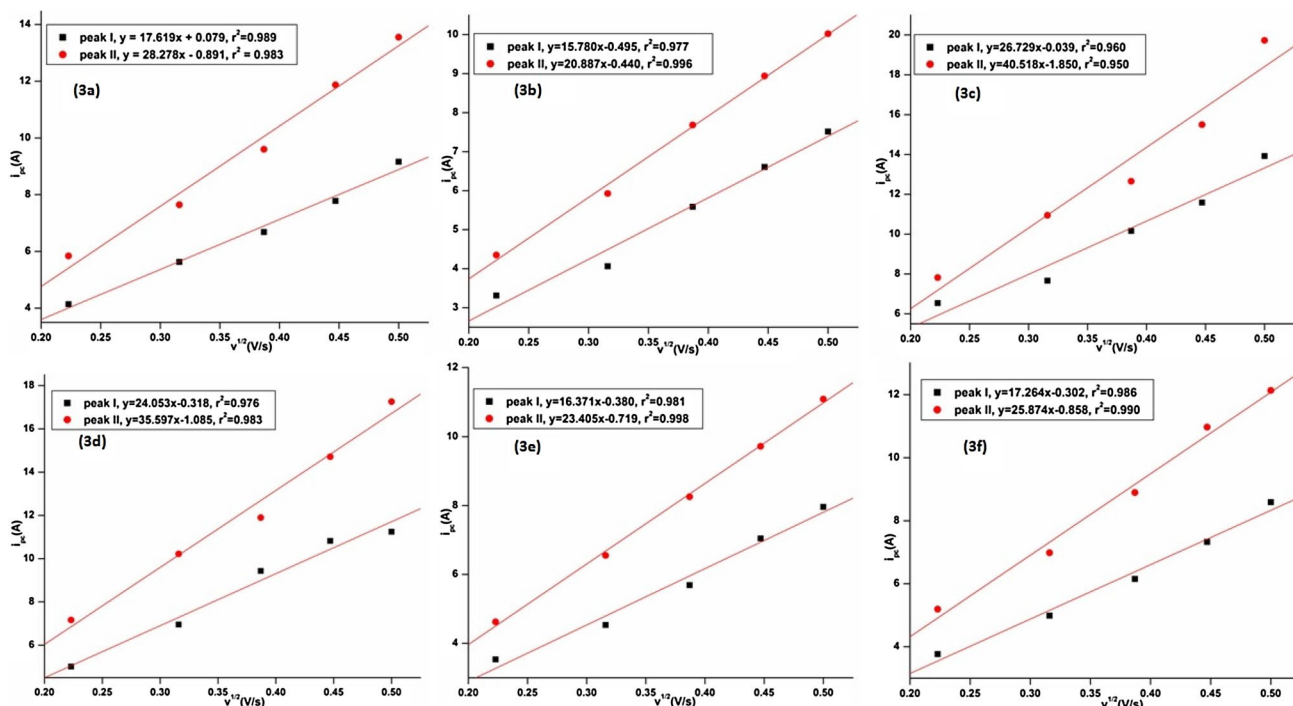
Table 2 Values of peak potential ($-E_{pc}$, V) and peak current (i_{pc}, A) of isonicotinoyl pyrazolyl derivatives (**3a–3f**) at different scan rates (pH 5.83, $C = 2.0 \times 10^{-4}$ M, $A = 0.081$ cm^2)

S. No	Compound	R	v (V/s)	$v^{1/2}$	$-E_{pc\ I}$ (V)	$-E_{pc\ II}$ (V)	$i_{pc\ I} \times 10^{-5}$ (A)	$i_{pc\ II} \times 10^{-5}$ (A)
1.	**3a**	H	0.05	0.223	0.738	1.239	4.140	5.842
			0.1	0.316	0.753	1.253	5.629	7.643
			0.15	0.387	0.763	1.261	6.683	9.602
			0.2	0.447	0.770	1.269	7.780	11.869
			0.25	0.5	0.776	1.278	9.162	13.552
2.	**3b**	4-F	0.05	0.223	0.725	1.226	3.311	4.348
			0.1	0.316	0.735	1.235	4.062	5.927
			0.15	0.387	0.745	1.239	5.585	7.683
			0.2	0.447	0.754	1.242	6.607	8.940
			0.25	0.5	0.763	1.248	7.516	10.023
3.	**3c**	4-CH$_3$	0.05	0.223	0.747	1.249	6.538	7.818
			0.1	0.316	0.766	1.266	7.662	10.942
			0.15	0.387	0.771	1.275	10.162	12.656
			0.2	0.447	0.778	1.277	11.584	15.500
			0.25	0.5	0.781	1.281	13.924	19.724
4.	**3d**	4-OCH$_3$	0.05	0.223	0.764	1.275	5.012	7.162
			0.1	0.316	0.781	1.291	6.954	10.218
			0.15	0.387	0.793	1.301	9.429	11.899
			0.2	0.447	0.801	1.311	10.823	14.710
			0.25	0.5	0.809	1.318	11.246	17.258
5.	**3e**	4-Cl	0.05	0.223	0.687	1.219	3.532	4.622
			0.1	0.316	0.695	1.225	4.531	6.551
			0.15	0.387	0.707	1.233	5.689	8.257
			0.2	0.447	0.715	1.235	7.047	9.722
			0.25	0.5	0.721	1.239	7.962	11.092
6.	**3f**	4-Br	0.05	0.223	0.662	1.216	3.767	5.192
			0.1	0.316	0.679	1.220	4.987	6.982
			0.15	0.387	0.682	1.226	6.152	8.893
			0.2	0.447	0.689	1.231	7.328	10.972
			0.25	0.5	0.697	1.235	8.590	12.134

Fig. 8 Plots of i_{pc} (A) vs $\nu^{1/2}$ (V/s) for all six derivatives at scan rate 0.05–0.25 V/s

Table 3 Linear equations for plot of log i_p vs log υ

S. No	Compound	Peak	Slope (variable is log ν)	Intercept	r^2
1	**3a**	I	0.480	− 0.206	0.992
		II	0.528	− 0.149	0.983
2	**3b**	I	0.526	− 0.340	0.967
		II	0.528	− 0.266	0.996
3	**3c**	I	0.471	− 0.012	0.949
		II	0.542	− 0.043	0.967
4	**3d**	I	0.532	− 0.205	0.985
		II	0.533	− 0.058	0.988
5	**3e**	I	0.512	− 0.342	0.979
		II	0.544	− 0.265	0.999
6	**3f**	I	0.506	− 0.298	0.987
		II	0.540	− 0.216	0.990

$$E_{p/2c}^{R} = \rho_R \times \sigma_R + E_{p/2c}^{H} \qquad (8)$$

where, $E_{p/2c}^{R}$ and $E_{p/2c}^{H}$ represent half peak potentials for substituted and unsubstituted derivatives, respectively, ρ_R is the specific rate constant and σ_R expressed Hammett constant for substituted derivatives.

A linear relationship between $E_{p/2c}$ and Hammett constants (σ) was obtained at pH 5.83 and a scan rate of 0.1 V/s. Figure 9 illustrates the correlation between half peak potential and Hammett constants for both the electroreduction processes. Figure 9 delineated that plots were straight lines with a positive slope and a good value of regression coefficient.

The linear equation obtained for two peaks are expressed as follows:

Table 4 Values of peak potential ($-E_{pc}$, V), half wave potential ($E_{p/2c}$, V) and charge transfer coefficient (α) for isonicotinoyl pyrazolyl derivatives (pH 5.83, $C = 2.0 \times 10^{-4}$ M, $\nu = 0.1$ V/s, $A = 0.081$ cm^2)

S. No	Compound	$-E_{pc\,I}$ (V)	$-E_{pc\,II}$ (V)	$E_{p/2c\,I}$ (V)	$E_{p/2c\,II}$ (V)	α_I	α_{II}
1.	1**3a**	0.745	1.253	0.654	1.160	0.524	0.513
2.	**3b**	0.712	1.235	0.613	1.139	0.482	0.497
3.	**3c**	0.766	1.266	0.671	1.175	0.502	0.524
4.	**3d**	0.781	1.291	0.689	1.197	0.518	0.507
5.	**3e**	0.695	1.225	0.598	1.127	0.492	0.487
6.	**3f**	0.679	1.220	0.589	1.125	0.530	0.502

$$E_{\text{p/2c}}^{\text{R}} = 0.188\,\sigma_{\text{R}} - 0.643\,\left(r^2 = 0.977\right)$$

$$E_{\text{p/2c}}^{\text{R}} = 0.132\sigma_{\text{R}} - 1.159\left(r^2 = 0.998\right)$$

The positive and low values of ρ indicated the nucleophilic addition of electrons to the substrates. This fact acknowledged the electron addition process to be the rate determining step in all the electro-reduction processes studied [31].

4 Plausible reduction mechanism

Keeping in view the feasible sites of reduction and based on cyclic voltammetric response (CV), the sites of reduction appeared to be the –C=N– of the pyrazoline ring and –C=O groups [30, 32]. There are two –C=O sites in the compound under investigation, considering the ease of reduction of carbonyl groups and the results obtained in the potential range of − 1.5 to + 1.5 V, the group attached to the pyrazoline ring was considered to be reduced (being a 3° linkage) in the process.

The cyclic voltammograms of the compound 3**c** have shown two reduction peaks pointing towards two reductive sites in the analyte. Further studies have shown the involvement of two and four electrons for the first and second reduction process, respectively. Moreover, the results from the Hammett equation justifies that, the transfer of electrons would be the rate-determining or slow step for both the reduction sites. The probable mechanism for reduction at ZnO-MWCNTs/GCE is depicted in Scheme 3.

5 Conclusion

The electrochemical studies at modified GCE (ZnO-MWC-NTs/GCE) for synthesized isonicotinoylpyrazolyl derivatives (3**a**–**f**) were found to be a promising tool to explore their electrochemical behavior. The fabricated sensor along with cationic surfactant (TEAP) exhibited an excellent electrocatalytic activity in enhancing the cathodic peak current and potential values as compared to bare GCE at pH 5.83. The remarkable activity of the sensor was attributed to the

Table 5 Diffusion-coefficient ($D_{\text{o}}^{1/2}$, cm^2/s) and forward rate constant (k^0, cm/s) for derivatives 3**a**–**f** (pH 5.83, $A = 0.081$ cm^2, $v = 0.10$ V/s, $C = 2 \times 10^{-4}$ M)

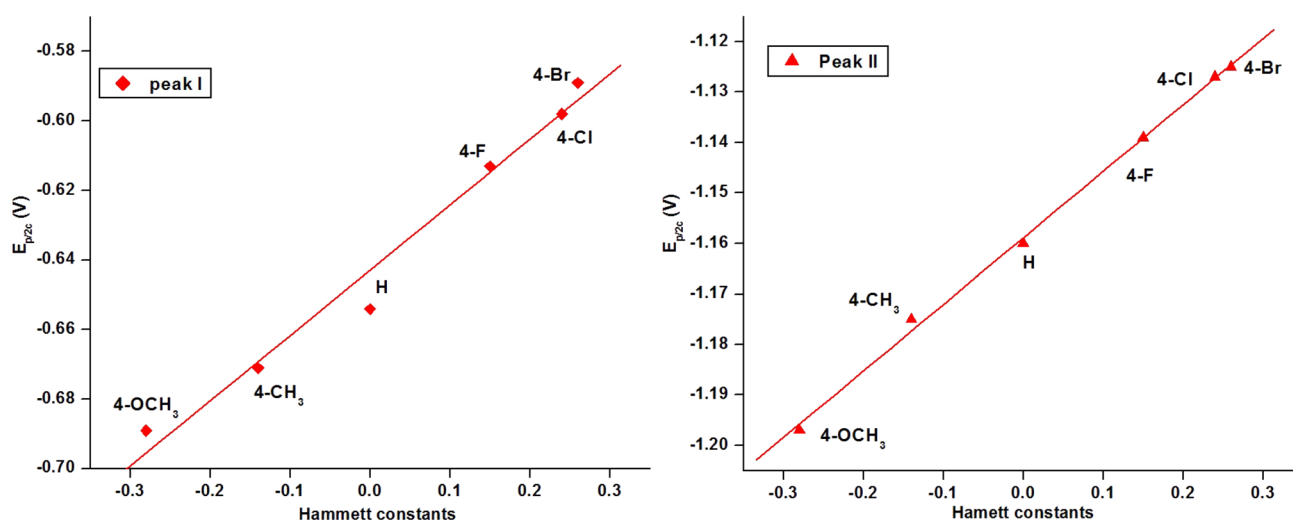| S. No	Compound	$D_0^{1/2} \times 10^{-5}$ for I peak	$D_0^{1/2} \times 10^{-5}$ for II peak	k° for I peak	k° for II peak
1.	3**a**	2.538	1.742	1.693×10^{-11}	7.325×10^{-16}
2.	3**b**	1.910	1.372	5.864×10^{-11}	1.755×10^{-15}
3.	3**c**	3.530	2.467	3.406×10^{-11}	4.703×10^{-16}
4.	3**d**	3.154	2.342	1.418×10^{-11}	6.197×10^{-16}
5.	3**e**	2.109	1.532	1.057×10^{-10}	3.792×10^{-15}
6.	3**f**	2.236	1.608	5.789×10^{-11}	2.179×10^{-15}

Fig. 9 Plots of $E_{\text{p/2c}}$ (V) *vs* Hammett substituents constant (σ) for isonicotinoylpyrazolyl derivatives (3**a**–**f**), at 2.0×10^{-4} M and 0.1 V/s of scan rate (v), on ZnO-MWCNTs/GCE (pH 5.83, $A = 0.081$ cm.^{2})
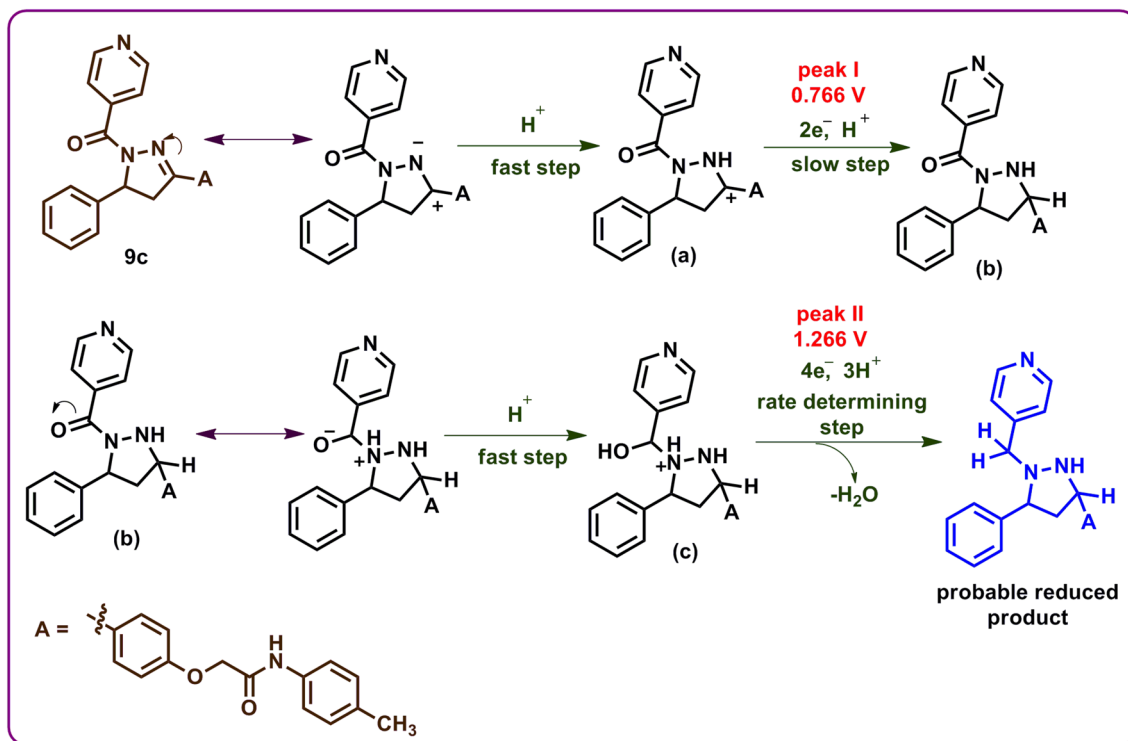
Scheme 3 Plausible electro-reduction mechanism of compound **3c**

synergistic effect of ZnO and MWCNTs and high cross-sectional surface area compared to unembellished GCE. The studies delineated the diffusion-controlled and irreversible behavior of electrocatalytic reaction for all the compounds under investigation. A sensitive electrochemical method using the modified GCE has been successfully employed for the first time for the detection of 2-(4-(1-isonicotinoyl-5-aryl-4,5-dihydro-1*H*pyrazol-3-yl)phenoxy)-*N*-arylacetamides. This sensor would be helpful for the determination and analysis of such type of compounds containing with high sensitivity and excellent selectivity.

Declarations

References

1. Kissinger PT, Heineman WR (1996) Laboratory techniques in electroanalytical chemistry, 2nd edn. Dekker, New York

2. Vittal R, Gomathi H, Kim KJ (2006) Beneficial role of surfactants in electrochemistry and in the modification of electrodes. Adv Colloid Interface Sci 119:55–68. https://doi.org/10.1016/j.cis.2005.09.004

3. Wang J (2000) Analytical electrochemistry, 2nd edn. Wiley, New York

4. Abdullah HM, Rania RZ, Esam AG, Mahmoud NAEl-Hady (2022) Bivalent transition metal complexes of pyridine-2,6-dicarbohydrazide: Structural characterization, cyclic voltammetry and biological studies. J Mol Struct 1269:133852. https://doi.org/10.1016/j.molstruc.2022.133852.

5. Kumar PS, Sreeja BS, Kumar KK, Padmalaya G (2022) Investigation of Nafion coated GO-ZnO nanocomposite behaviour for sulfamethoxazole detection using cyclic voltammetry. Food Chem Toxicol 167:113311. https://doi.org/10.1016/j.fct.2022.113311.

6. Gupta VK, Jain R, Radhapyari K, Jadon N, Agarwal S (2011) Voltammetric techniques for the assay of pharmaceuticals—a review. Anal Biochem 408:179–196. https://doi.org/10.1016/j.ab.2010.09.027

7. Ghassab N, Soleymanpour A, Shafaatian B (2022) Development of an ultrasensitive chemically modified carbon paste electrode for

selective determination trace amount of sulfate ion. Measurement 205:112231. https://doi.org/10.1016/j.measurement.2022.112231.

8. Zare HR, Nasirizadeh N (2010) Simultaneous determination of ascorbic acid, adrenaline and uric acid at a hematoxylin multi-wall carbon nanotube modified glassy carbon electrode. Sens Actuators B 143:666–672. https://doi.org/10.1016/j.snb.2009.10.030

9. Carmichael AJ, Seddon KR (2000) Polarity study of some 1-alkyl-3-methylimidazolium ambient-temperature ionic liquids with the solvatochromic dye, Nile Red. J Phys Org Chem 13:591–595

10. Shrivastava S, Jadon N, Jain R (2016) Next-generation polymer nanocomposite-based electrochemical sensors and biosensors: a review. Trends Analt Chem 82:55–67. https://doi.org/10.1016/j.trac.2016.04.005

11. Zhang C, Wang G, Liu M, Feng Y, Zhang Z, Fang B (2010) A hydroxylamine electrochemical sensor based on electrodeposition of porous ZnO nanofilms onto carbon nanotubes films modified electrode. Electrochim Acta 55:2835–2840. https://doi.org/10.1016/j.electacta.2009.12.068

12. Maheshwaran S, Tamilalagan E, Chen S-M, Akilarasan M, Huang Y-F, AlMasoud N, Abualnaja KM, Ouladsmne M (2021) Rationally designed f-MWCNT-coated bismuth molybdate (f-MWCNT@BMO) nanocomposites for the voltammetric detection of biomolecule dopamine in biological samples. Microchim Acta 188:315. https://doi.org/10.1007/s00604-021-04978-9

13. Jain R, Sharma RK (2012) Novel bismuth/multi-walled carbon nanotubes-based electrochemical sensor for the determination of neuroprotective drug cilostazol. J Appl Electrochem 42:341–348. https://doi.org/10.1007/s10800-012-0402-8

14. Periasamy AP, Yang S, Chen SM (2011) Preparation and characterization of bismuth oxide nanoparticles-multiwalled carbon nanotube composite for the development of horseradish peroxidase based H2O2 biosensor. Talanta 87:15–23. https://doi.org/10.1016/j.talanta.2011.09.021

15. Jiang LC, Zhang WD (2009) Electrodeposition of TiO$_2$ nanoparticles on multiwalled carbon nanotube arrays for hydrogen peroxide sensing. Electroanalysis 21:988–993. https://doi.org/10.1002/elan.200804502

16. Gupta VK, Jain R, Agarwal S, Mishra R, Dwivedi A (2011) Electrochemical determination of antihypertensive drug irbesartan in pharmaceuticals. Anal Biochem 410:266–271. https://doi.org/10.1016/j.ab.2010.11.024

17. Arun V, Prabhu S, Priyadharsan A, Maadeswaran P, Sohila S, Ramesh R, Kumar AS (2021) Facile, low cost synthesis of cauliflower-shaped ZnO with MWCNT/rGO nanocomposites and their photocatalytic activity. J Mater Sci: Mater Electron 32:15763–15777. https://doi.org/10.1007/s10854-021-06129-5

18. Prabhu K, Malode SJ, Shetti NP, Kulkarni RM (2022) Analysis of herbicide and its applications through a sensitive electrochemical technique based on MWCNTs/ZnO/CPE fabricated sensor. Chemosphere 287: 132086. https://doi.org/10.1016/j.chemosphere.2021.132086.

19. Westmoreland PG, Day RA, Underwood AL (1972) Electrochemistry of substances solubilized in micelles. Polarography of azobenzene in aqueous surfactant solutions. Anal Chem 44:737–740. https://doi.org/10.1021/ac60312a060

20. Ziyatdinova G, Giniyatova E, Budnikov H (2010) Cyclic voltammetry of retinol in surfactant media and its application for the analysis of real samples. Electroanalysis 22:2708–2713. https://doi.org/10.1002/elan.201000358

21. Jain R, Dwivedi A, Mishra R (2009) Adsorptive stripping voltammetric behavior of nortriptyline hydrochloride and its determination in surfactant media. Langmuir 25:10364–10369. https://doi.org/10.1021/la900927j

22. Levent Y, Yardim Z, Senturk, (2009) Voltammetric behavior of nicotine at pencil graphite electrode and its enhancement determination in the presence of anionic surfactant. Electrochim Acta 55:190–195. https://doi.org/10.1016/j.electacta.2009.08.035

23. Elgrishi NM, Rountree KJ, McCarthy BD, Rountree ES, Eisenhart TT, Dempsey JL (2018) A practical beginner's guide to cyclic voltammetry. J Chem Educ 95:197–206. https://doi.org/10.1021/acs.jchemed.7b00361

24. Ma L, Xie C, Ma Y, Liu J, Xiang M, Ye X, Zheng H, Chen Z, Xu Q, Chen T, Chen J, Yang J, Qiu N, Wang G, Liang X, Peng A, Yang S, Wei Y, Chen L (2011) Synthesis and biological evaluation of novel 5-benzylidenethiazolidine-2,4-dione derivatives for the treatment of inflammatory diseases. J Med Chem 54:2060–2068. https://doi.org/10.1021/jm1011534

25. Reen GK, Ahuja M, Kumar A, Patidar R, Sharma P (2017) ZnO nanoparticle-catalyzed multicomponent reaction for the synthesis of 1,4-diaryl dihydropyridines. Org Prep Proced Int 49:273–286. https://doi.org/10.1080/00304948.2017.1320927

26. Jain R, Sinha A, Kumari N, Khan AL (2016) A polyaniline/graphene oxide nanocomposite as a voltammetric sensor for electroanalytical detection of clonazepam. Anal Methods 8:3034–3045. https://doi.org/10.1039/c6ay00424e

27. Murugan N, Kumar THV, Devi R, Sundramoorthy AK (2019) A flower-structured MoS$_2$-decorated f-MWCNTs/ZnO hybrid nanocomposite-modified sensor for the selective electrochemical detection of vitamin C. New J Chem 43:15105–15114. https://doi.org/10.1039/c9nj02993a

28. Britton HTS (1956) Hydrogen ions, vol I. Van Nostrand Co., New York

29. Bard AJ, Faulkner LR (2010) Electrochemical methods: fundamentals and applications. Wiley, New York

30. Abou-Elenien GM, Ismail NA, El-Maghraby AA, Al-abdallah GM (2001) Electrochemical studies on some pyrazole, oxadiazole, and thiadiazole derivatives. Electroanalysis 13:1022–1029. https://doi.org/10.1002/1521-4109(200108)13:12%3C1022::aid-elan1022%3E3.0.co;2-x

31. Kumar KR, Prasad ARG, Srilalitha V, Swamy GN, Ravindranath LK (2012) Synthesis and electrochemical investigations on certain pyrazolin-5-ones. Scientica Iranica 19:605–618. https://doi.org/10.1016/j.scient.2012.02.025

32. Beloglazkina EK, Korablina DD, Vorozhtsov NI, Sviridova LA, Moiseeva AA, Skvortsov DA, Rybakov VB, Majouga AG, Zyk NV (2019) Synthesis of 3-(pyridine-2-yl)-4,5-dihydro-1H-pyrazole-1-thiocarboxamides and their copper(II) complexes. Arab J Chem 12:1050–1060. https://doi.org/10.1016/j.arabjc.2017.01.005